Isotropic AVO Methods to Detect Fracture-Prone Zones in Tight Gas Resource Plays*

Bill Goodway[1], John Varsek[1], and Christian Abaco[1]

Search and Discovery Article #41584 (2015)
Posted March 9, 2015

*Adapted from extended abstract prepared for presentation at CSPG CSEG GeoConvention 2007, Calgary, Alberta, Canada, May 14-17, 2007, Datapages/CSPG © 2015. Please refer to companion article, Search and Discovery Article #41531 (2015).

[1]EnCana Corp., Calgary, AB, Canada, (william.goodway@encana.com)

Introduction

Exploration and drilling for natural gas in North America has moved radically away from conventional reservoirs to focus on unconventional reservoirs such as coal bed methane (CBM), tight gas sands and shales. These reservoirs, termed Resource Plays at EnCana, are low permeability-porosity reservoirs with gas stored in natural fractures or cleats and within the matrix porosity. Due to low permeability, economic gas production can only be achieved through hydraulic fracture stimulation. Effective stimulation requires either the opening of a connection to existing natural fractures or the presence of geo-mechanical brittleness within the formation capable of supporting extensive induced fractures. Despite adequate stimulation significant variations exist between wells in stabilized gas rates and economic ultimate recovery due to the heterogeneity of these Resource Plays. Consequently, predicting natural fractures or fracture prone "sweet spots" is essential to the successful development of such plays.

Seismic 3D, AVO and AVO variation with azimuth (AVAZ) to detect anisotropy due to fractures or stress, offer the only opportunity to directly identify "sweet spots" prior to committing to significant horizontal well drilling costs. This article describes the rock mechanics and conventional isotropic AVO that can be applied to map Resource Play potential and predict optimal drilling locations.

Mechanical Characteristics of Tight Gas Reservoirs using Seismic Petrophysics

As tight gas Resource Plays have low porosity/permeability and are generally fully gas charged, the application of AVO and AVAZ methods is simplified to primarily extracting lithologic and mechanical properties from seismic data. Examples of this analysis are shown for the gas shale case, but the methods are equally applicable to CBM or tight gas sands.

Engineering literature for the Barnett gas shales focuses on identifying optimum mechanical properties of Young's modulus (E) and Poisson's ratio (ν) as shown in Figure 1 (Grigg, 2004). In order to better understand the significance of E and ν, these parameters are converted to the simpler and more seismically intuitive Lamé parameters of incompressibility Lambda (λ) and rigidity Mu (μ) (Goodway et al., 1997, 2001) through the following relationships:

$$M = \lambda + 2\mu \qquad \text{P - wave propagation and bound uniaxial compression modulus}$$

$$E = \frac{\mu(3\lambda + 2\mu)}{\lambda + \mu} = M - 2\lambda\nu \qquad \text{Un - bound uniaxial compression modulus}$$

$$\nu = \frac{\lambda}{2(\lambda + \mu)}$$

From above E and ν can be related as:

$$\frac{E}{1+\nu} = 2\mu$$

An initial observation is that the inverse linear relation between increasing E to decreasing shown for the Barnett Shale in Figure 1, is simply the result of an increase in rigidity μ.

By using the relationships above, a cross-plot graph can be constructed showing Young's modulus vs. Lambda with curves of constant Mu and lines of constant Poisson's ratio (Figure 2). The graph shows further physical insight for the extended Barnett Shale trend, with a clear division into brittle and ductile zones having a Mu cutoff of between 4 to 8 G.Pa. This cross-plot is used as a template to guide the seismic petrophysics and AVO expectation to identify similar gas shales. Log data from various lithologies in the WCSB can be compared to the Barnett Shale as shown in Figure 3. From the four zones shown only the Nordegg has similar λ, μ values to the Barnett Shale. By contrast the Colorado/SWS group's highest μ rigidity values of 5-6 G.Pa (red points) are lower by a factor of two from the Barnett Shale, but have a similar λ range.

Despite this, the conclusion of requiring as high a Mu or MuRho (μρ) parameter as possible to support natural or induced fractures is still a viable criterion for use in the 3D seismic AVO/LMR (Lambda, Mu, Rho) analysis. Interpretation of the λ, μ cross-plots suggest the best zones appear to occupy areas more commonly associated with low porosity lithic gas sands, shown in conventional log-based LMR templates (Goodway et al., 2001, 2006). This is not surprising considering the reason for the Barnett Shale's ability to support natural or induced fractures (fracablity) is due to its unusually high quartz content for a shale. From an engineering perspective a rock's fracablity is given by the Warpinski closure stress equation as a function of E and ν (eqn.1 below), hence the Barnett Shale emphasis on these properties.

$$\sigma_{xx} = \frac{\nu}{1-\nu}\left[\sigma_{zz} - B_V P_P\right] + B_H P_p + \frac{E}{1-\nu^2}\left(e_{xx} + \nu e_{yy}\right) \qquad \text{eqn(1) after Warpinski}$$

where σ_{xx} = horizontal (closure) stress, σ_{zz} = overburden stress, e_{xx}, e_{yy}, e_{zz} = strains in x, y and z

P_P = pore pressure, B_V and B_H = vertical and horizontal poro - elastic constant

In a similar manner used to convert E and ν to λ and μ, the closure stress equation can be written in seismically familiar Lamé terms:

$$\sigma_{xx} = \frac{\lambda}{\lambda + 2\mu}\left[\sigma_{zz} - B_V P_P + 2\mu\left(\frac{e^2{}_{yy} - e^2{}_{xx}}{e_{yy}}\right)\right] + B_H P_p \qquad \text{eqn(2)}$$

Now the most fracable zones occupying relatively low λ's and high μ's in the cross-plots above, can be understood as also having the lowest closure stress, governed by the λ/(λ+2μ) ratio term in equation 2. Furthermore, the tectonic strain's (eyy,exx) last term in the box bracket, is simply the rock's anisotropy given as the % difference in maximum-minimum strain energy (potential) from tectonic stresses. This term has a direct relationship to seismic AVAZ measurements. Finally the basic influence of λ and μ on horizontal closure stress is captured in diagram A, where rigidity Mu determines the rock's resistance to transverse or shear failure and Lambda is the rock's resistance to fracture dilation that in turn relates to pore pressure.

Diagram A.

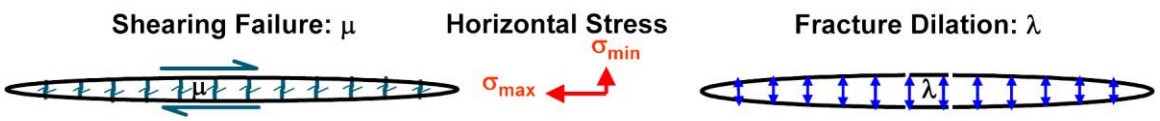

Mechanical Properties and Fracture Detection from Seismic AVO/LMR

The 3D survey used in the AVO-AVAZ case study was optimally acquired with a wide-azimuth, high-density far-offset MegaBin acquisition (Goodway, Ragan, and Li, 1996) that resulted in an exceptionally good analysis of offset and azimuth AVO variations. An azimuth-offset gather from the 3D shown in Figure 4 has a good AVO type 1 and 2 match for zones of high MuRho rigidity contrast, at both the top of the Colorado B and within the 2nd White Specks, that might support potential natural or induced fractures based on the mechanical or elastic attribute log analysis, described above.

The LMR cross-plot and polygon section, shown in Figures 5a and 5b, are from a 3D cross-line that ties the control well log. In this interpretation the highest μρ and lowest λρ zones are clearly isolated at the top Colorado B at ~ 425 ms and mid to base 2nd White Specks at 450-500 ms, by the red LMR cross-plot polygon. The Colorado B zone also has a few very high MuRho values (yellow cross-plot polygon points left of blue arrow in Figure 5b) that approach those of the Barnett Shale analogue.

Conclusions

This article describes the potential of conventional isotropic AVO to identify optimum geo-mechanical properties for the successful exploitation of tight gas shale Resource Plays through effective hydraulic fracture stimulation. Based on comparisons to the Barnett Shale, the optimum gas shale properties have relatively low λ's (incompressibility) and high μ's (rigidity) that give rise to geo-mechanical brittleness capable of supporting extensive induced fractures. Furthermore, these properties also produce the lowest closure stresses (i.e., largest fractures) due to the $\lambda/(\lambda+2\mu)$ ratio term in the closure stress equation. The isotropic AVO modelling based on logs tied to 3D data indicate that shale zones have mostly type 1 AVO responses, i.e., high shear-wave impedance, that best matched the Barnett Shale analogue. A successful deviated well was located by identifying the most fracture-prone high MuRho zones, combined with faulting implied from 3D coherence attribute lineations along with an AVAZ fracture intensity and orientation volume. The resulting combined attribute volume using independent parameter estimates provided powerful corroborative evidence of areas with the best probability of high fracture intensity or “fracability” and good gas charge.

References Cited

Grigg, M., 2004, Emphasis on mineralogy and basin stress for shale gas exploration: SPE meeting on Gas Shale Technology Exchange.

Goodway, W., 2001 AVO and Lamé constants for rock parameterization and fluid detection: CSEG Recorder June 2001, p. 39-60.

Goodway, W., T. Chen, and J. Downton, 1997, Improved AVO fluid detection and lithology discrimination using Lamé parameters; λρ, μρ and λ/μ fluid stack from P and S inversions: CSEG Convention Expanded Abstracts, p. 148-151.

Goodway, W., B. Ragan, and G. Li, 1996, Mega-Bin Land 3D Seismic: Toward a cost effective "symmetric patch geometry" via regular spatial sampling in acquisition design & cooperative processing, for significantly improved S/N & resolution: CSEG National Convention Expanded Abstracts.

Goodway, W., J. Varsek, and C. Abaco, 2006, Practical applications of P-wave AVO for unconventional gas Resource Plays-1: Seismic petrophysics: CSEG Recorder, v. 31, Special Edition March, 2006, p. 90-95.

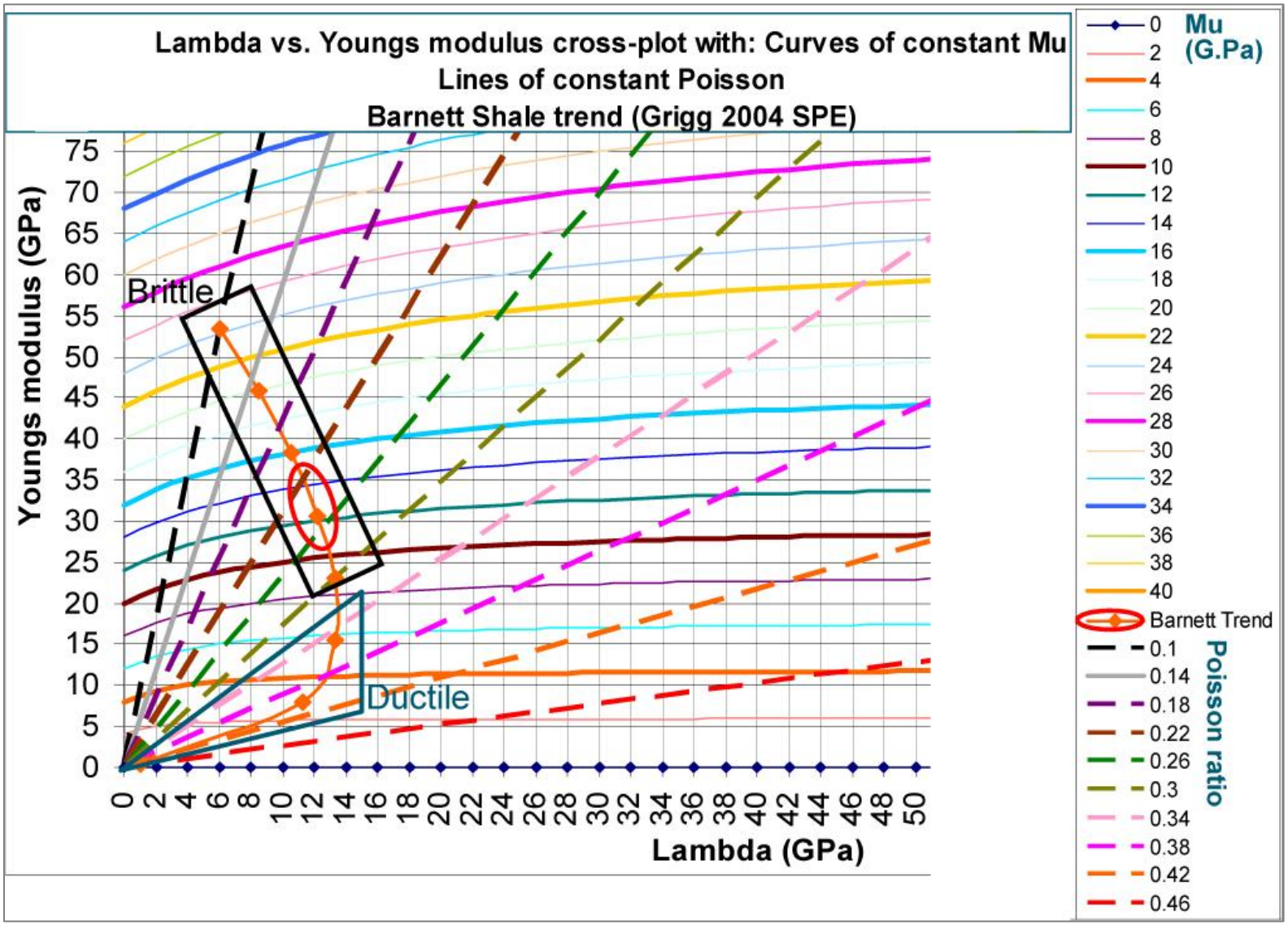

Figure 1. Relationship of Young's modulus to Poisson ratio for the Barnett Shale (Grigg, 2004).

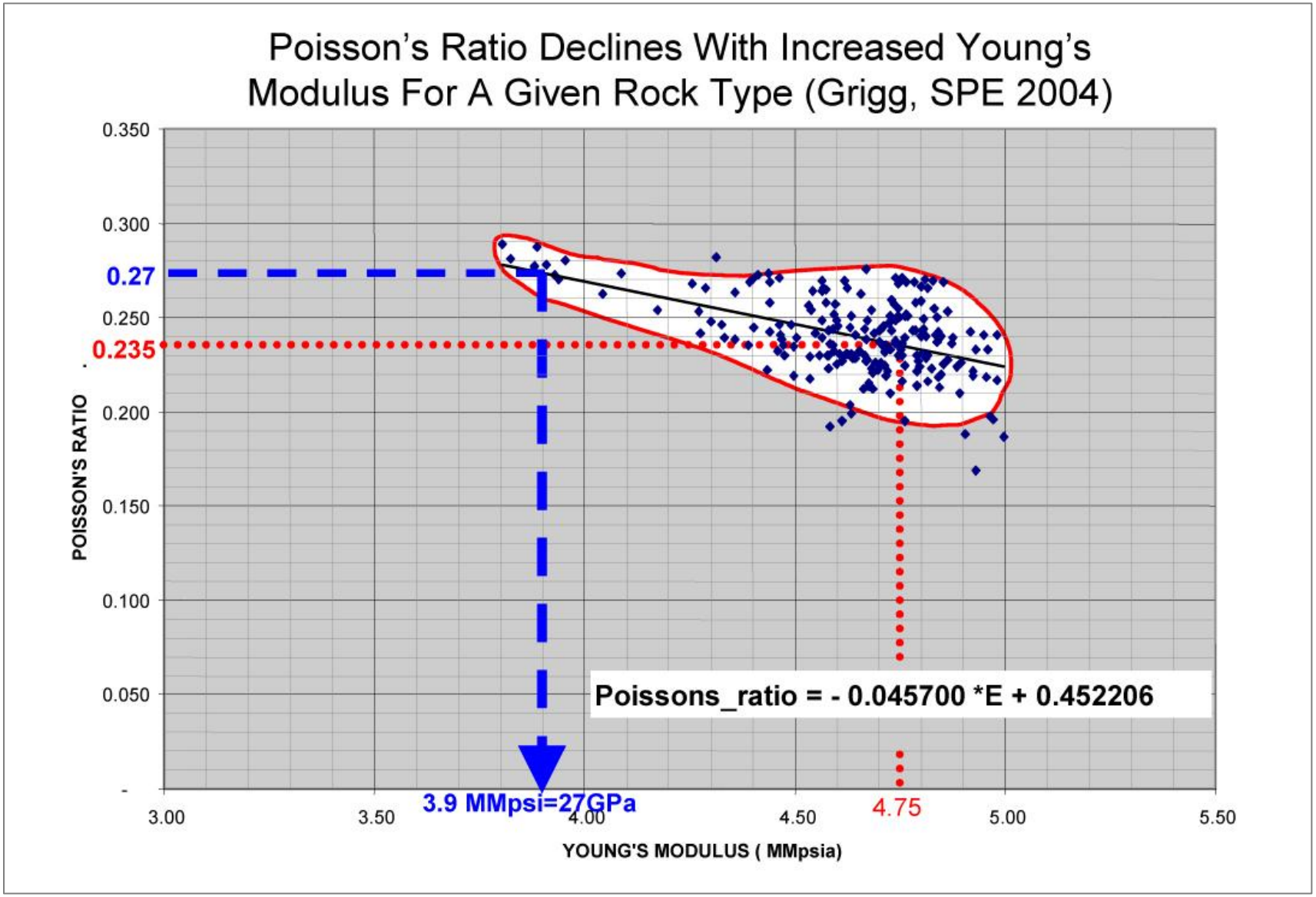

Figure 2. Lambda vs. Young's modulus relationship with curves of constant Mu and lines of constant Poisson's ratio (extended Barnett Shale trend equation from Grigg (2004) is also shown as the orange curve overlay with ductile and brittle zones).

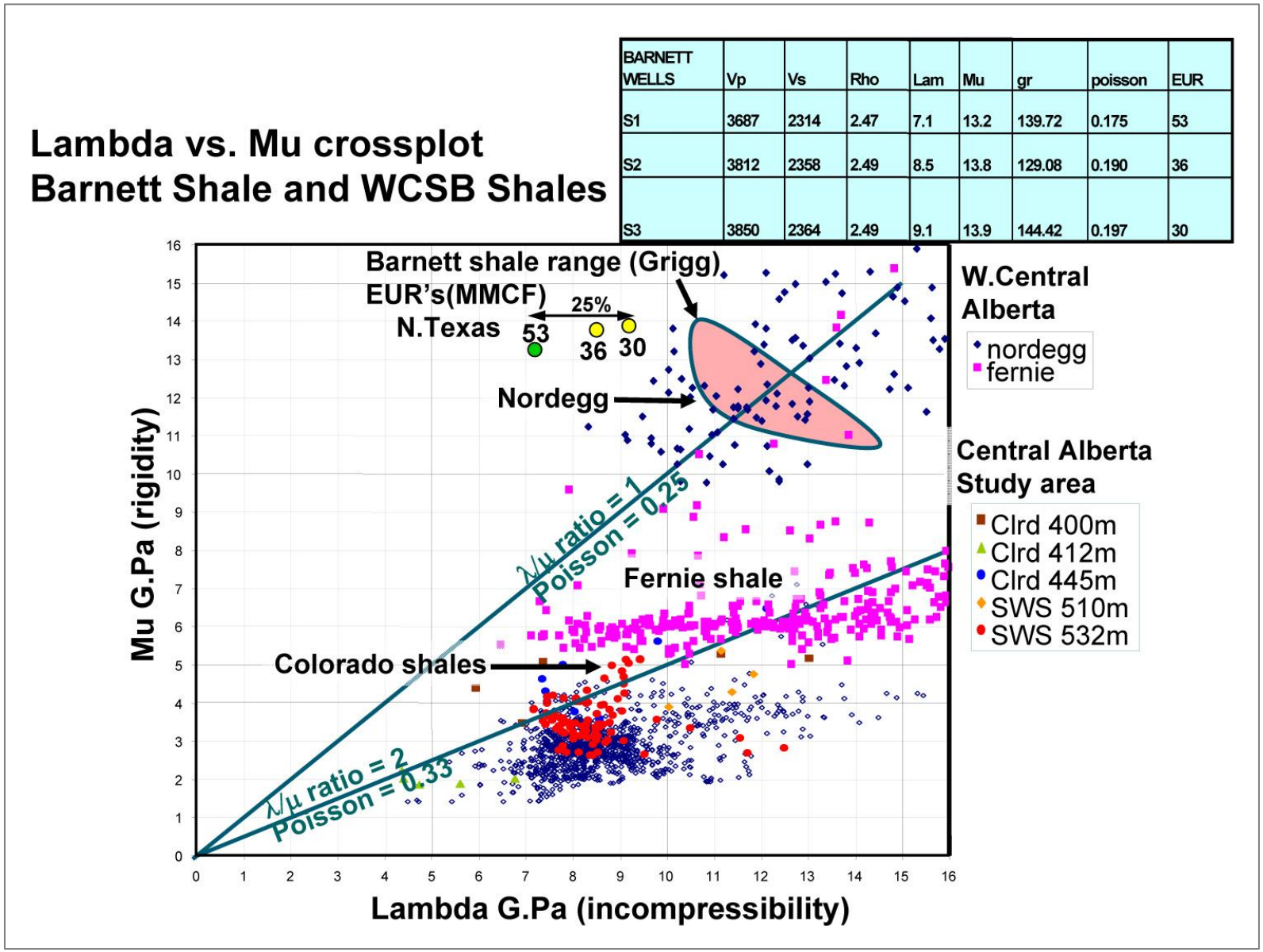

BARNETT WELLS	Vp	Vs	Rho	Lam	Mu	gr	poisson	EUR
S1	3687	2314	2.47	7.1	13.2	139.72	0.175	53
S2	3812	2358	2.49	8.5	13.8	129.08	0.190	36
S3	3850	2364	2.49	9.1	13.9	144.42	0.197	30

Figure 3. Lambda vs. Mu cross-plot comparing various shales from the WCSB to the Barnett Shale.

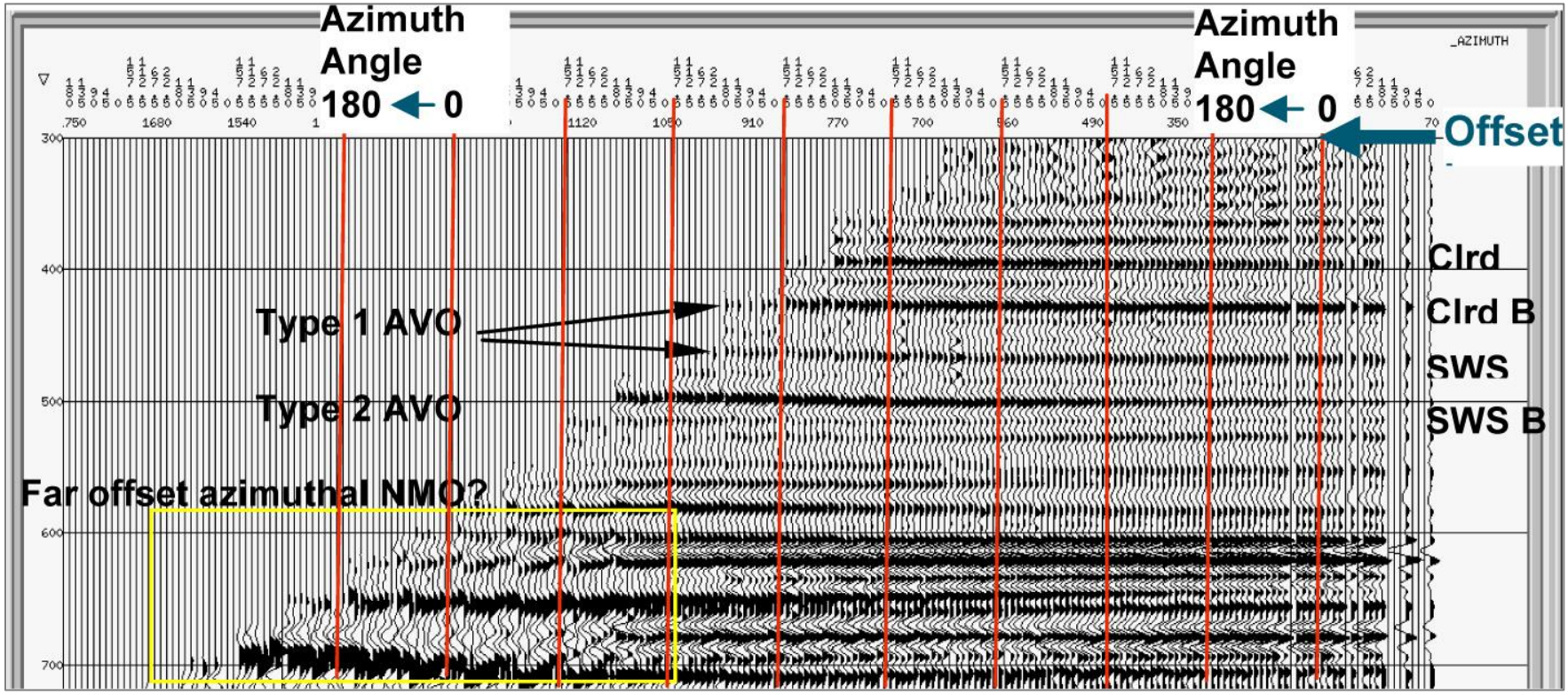

Figure 4. Azimuth-offset gather from 3D confirms model predictions for an AVO type 1, 2 response at the Colorado B, and 2nd White Specks zones (Clrd B, SWS).

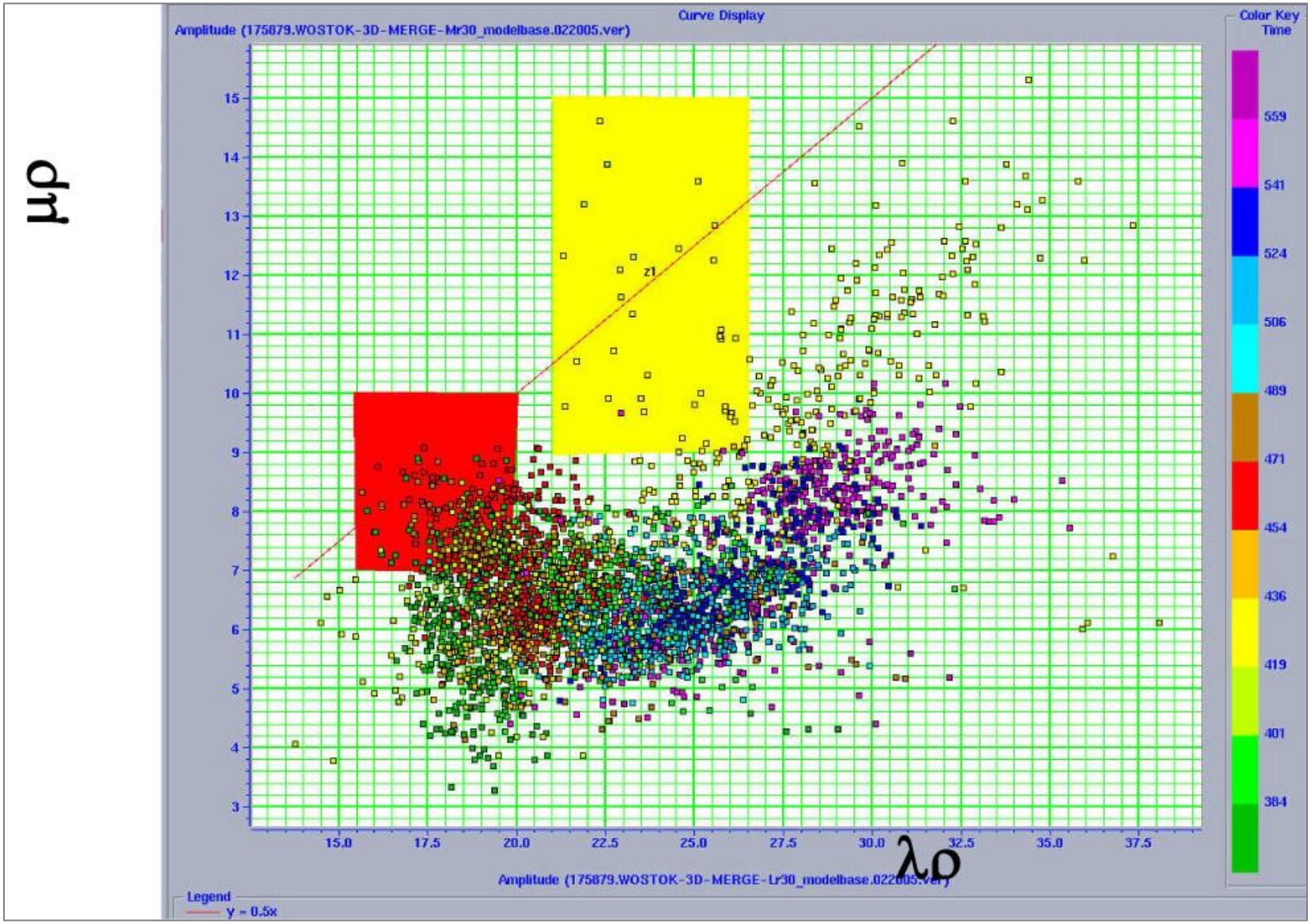

Figure 5a. LMR cross-plot and selected polygons for 3D line shown in Figure 5b.

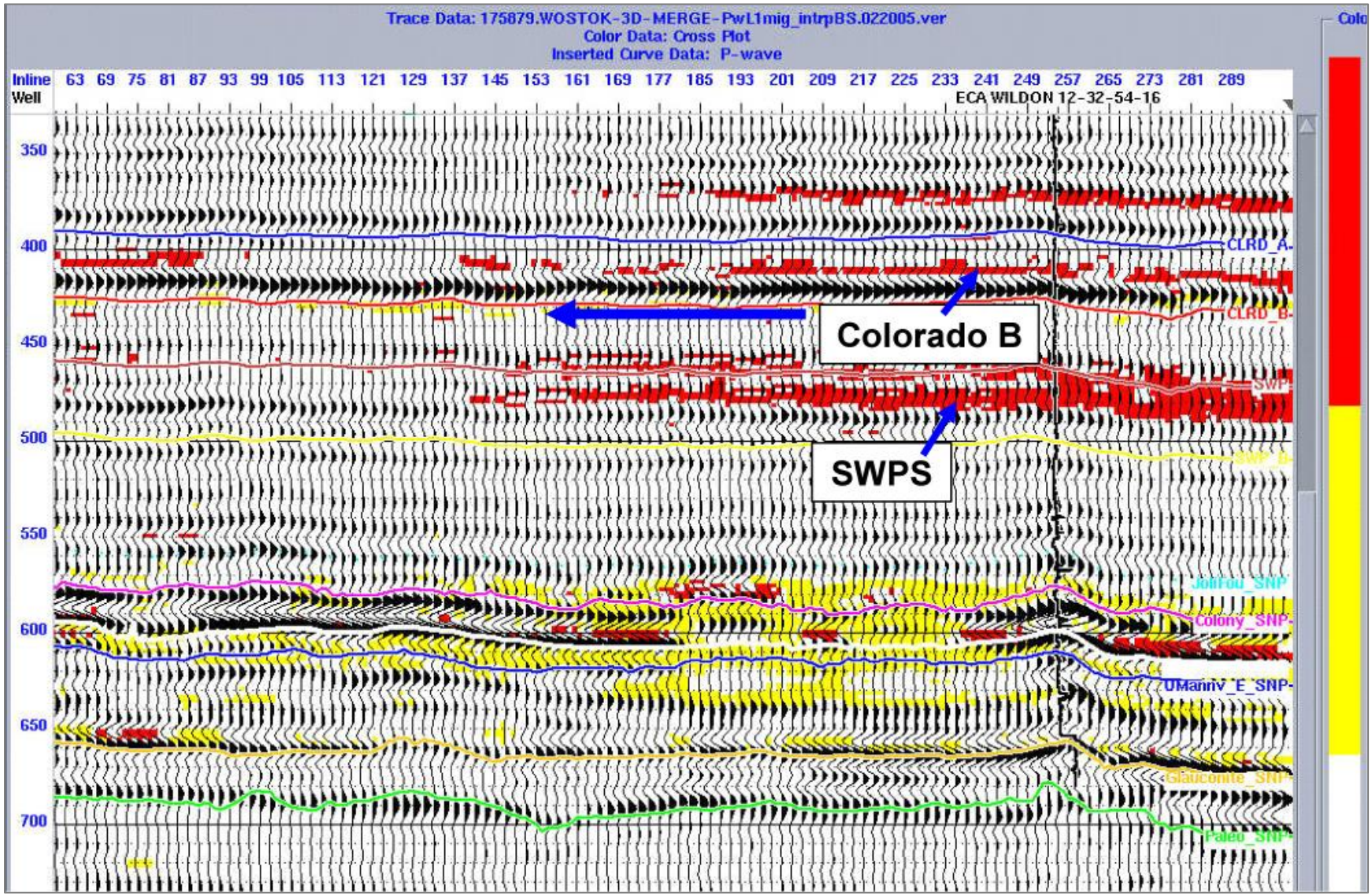

Figure 5b. Result of LMR cross-plot polygon mask from Figure 5a, for a cross-line from 3D case study.